ortho-Bis(cyanomercurio)tetrafluorobenzene as a Bidentate Lewis Acid Co-catalyst in the Cyanosilylation of Benzaldehyde

Julie B. King and François P. Gabbaï*

Chemistry Department, Texas A&M University, 3255 TAMU, College Station, Texas 77843-3255

Received November 5, 2002

Reaction of *o*-$C_6F_4(HgCl)_2$ (**1**), *m*-$C_6F_4(HgCl)_2$ (**2**), C_6F_5HgCl (**3**), and $C_6F_4H(HgCl)$ (**4**) with TMSCN in MeCN affords the corresponding organomercury cyanide derivatives *o*-$C_6F_4(HgCN)_2$ (**5**), *m*-$C_6F_4(HgCN)_2$ (**6**), C_6F_5HgCN (**7**), and $C_6F_4H(HgCN)$ (**8**), respectively. These compounds have been characterized by elemental analysis, ^1H, ^{13}C, ^{19}F, and ^{199}Hg NMR, and IR spectroscopy. The infrared spectra of **5**−**8** display a cyanide stretching band in the range 2170−2183 cm^{-1}, while their ^{199}Hg NMR chemical shifts are all within the range −1170 to −1250 ppm. The crystal structures of [**2**·DMF], [**5**·MeCOH], [**5**·PhCOH], and **8** have been determined. In [**2**·DMF], the DMF molecule acts as a terminal ligand and coordinates one of the mercury centers through the formation of a Hg−O bond of 2.746(14) Å. A similar situation is encountered in [**5**·MeCOH] and [**5**·PhCOH], wherein the aldehyde ligand is terminally ligated to one of the mercury centers through a Hg−O bond of 2.855(19) and 3.009(12) Å, respectively. In these compounds, the neighboring molecules engage in long intermolecular Hg···N contacts. In [**5**·MeCOH], these interactions lead to the formation of a hexameric aggregate whose shape is reminiscent of a capsule. The ability of **5**−**8** to catalyze the cyanosilylation of benzaldehyde has been studied. While little or no product formation is observed when the pure cyanide derivatives **5**−**8** are employed as catalysts, their combination with TMSCl leads to the formation of active catalytic species. The combination of bidentate **5** and TMSCl provides the most active system. The results are rationalized on the basis of a working model in which TMSCl is activated by the halophilic bidentate fluorinated mercury derivative **5**, which produces a catalytically active Lewis acidic silicon species.

Introduction

The multiple coordination of halide anions by polydentate Lewis acids is a rapidly growing area of chemistry.[1−7] At the fundamental level, this chemistry has led to the isolation of complexes with unprecedented coordination numbers and environments at the anion.[8−10] As a result of cooperative effects, such complexes often display an enhanced stability when compared to complexes involving single-site Lewis acids.[11] These observations have led to the development of a new generation of Ziegler−Natta metallocene olefin polymerization activators.[12−17] In particular, bidentate boranes have proved useful for the generation of a metallocenium salt in which the anion consists of a chelate complex involving bidentate boranes.[12,17] Due to the sharing of the negative charge over two borate centers, the chelate

* To whom inquiries about the paper should be addressed.

(1) Hawthorne, M. F. *Pure Appl. Chem.* **1994**, *66*, 245−254. Hawthorne, M. F.; Zheng, Z. *Acc. Chem. Res.* **1997**, *30*, 267−276.
(2) Chistyakov, A. L.; Stankevich, I. V.; Gambaryan, N. P.; Struchkov, Y. T.; Yanovsky, A. I.; Tikhonova, I. A.; Shur, V. B. *J. Organomet. Chem.* **1997**, *536*, 413−424.
(3) Vaugeois, J.; Simard, M.; Wuest, J. D. *Coord. Chem. Rev.* **1995**, *145*, 55−73.
(4) Katz, H. E. *Inclusion Compd.* **1991**, *4*, 391.
(5) Piers, W. E.; Irvine, G. J.; Williams, V. C. *Eur. J. Inorg. Chem.* **2000**, *10*, 2131.
(6) Chen, E. Y.-X.; Marks, T. J. *Chem. Rev.* **2000**, *100*, 1391−1434.
(7) For recent reviews see: (a) Kaufmann, D. E.; Otten, A. *Angew. Chem.* **1994**, *106*, 1917−1918. (b) Schmidtchen, F. P.; Berger, M. *Chem. Rev.* **1997**, *97*, 1609−1646. (c) Beer, P. D.; Smith, D. K. *Prog. Inorg. Chem.* **1997**, *46*, 11−96. (d) Antonisse, M. M. G.; Reinhoudt, D. N. *Chem. Commun.* **1998**, 443−448. (e) Beer, P. D.; Gale, P. A. *Angew. Chem., Int. Ed.* **2001**, *40*, 486-516.
(8) (a) Shur, V. B.; Tikhonova, I. A.; Yanovskii, A. I.; Struchkov, Y. T.; Petrovskii, P. V.; Panov, S. Y.; Furin, G. G.; Vol'pin, M. E. *J. Organomet. Chem.* **1991**, *418*, C29−C32. (b) Shur, V. B.; Tikhonova, I. A.; Yanovskii, A. I.; Struchkov, Y. T.; Petrovskii, P. V.; Panov, S. Y.; Furin, G. G.; Vol'pin, M. E. *Dokl. Akad. Nauk SSSR* **1991**, *321*, 1002−1004. (c) Shur, V. B.; Tikhonova, I. A.; Dolgushin, F. M.; Yanovsky, A. I.; Struchkov, Y. T.; Volkonsky, A. Y.; Solodova, E. V.; Panov, S. Y.; Petrovskii, P. V.; Vol'pin, M. E. *J. Organomet. Chem.* **1993**, *443*, C19−C21.
(9) Wuest, J. D.; Zacharie, B. *Organometallics* **1985**, *4*, 410−411.
(10) Lee, H.; Diaz, M.; Knobler, C. B.; Hawthorne, M. F. *Angew. Chem., Int. Ed.* **2000**, *39*, 776−778.
(11) Katz, H. E. *J. Org. Chem.* **1985**, *50*, 5027−5032.
(12) Jia, L.; Yang, X.; Stern, C.; Marks, T. J. *Organometallics* **1994**, *13*, 3755−3757.
(13) Metz, M. V.; Schwartz, D. J.; Stern, C. L.; Nickias, P. N.; Marks, T. J. *Angew. Chem., Int. Ed.* **2000**, *39*, 1312−1316.
(14) Köhler, K.; Piers, W. E.; Jarvis, A. P.; Xin, S.; Feng, Y.; Bravakis, A. M.; Collins, S.; Clegg, W.; Yap, G. P. A.; Marder, T. B. *Organometallics* **1998**, *17*, 3557−3566.
(15) Williams, V. C.; Piers, W. E.; Clegg, W.; Elsegood, M. R. J.; Collins, S.; Marder, T. B. *J. Am. Chem. Soc.* **1999**, *121*, 3244−3245.
(16) Williams, V. C.; Dai, C.; Li, Z.; Collins, S.; Piers, W. E.; Clegg, W.; Elsegood, M. R. J.; Marder, T. B. *Angew. Chem., Int. Ed.* **1999**, *38*, 3695−3698.
(17) Williams, V. C.; Irvine, G. J.; Piers, W. E.; Li, Z.; Collins, S.; Clegg, W.; Elsegood, M. R. J.; Marder, T. B. *Organometallics* **2000**, *19*, 1619−1621.

10.1021/om020918u CCC: $25.00
Publication on Web 02/15/2003

Scheme 1

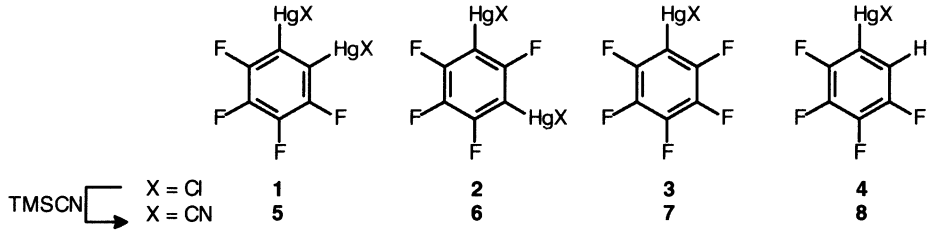

anionic complexes are weakly coordinating, which leads to the formation of very active metallocenium catalysts. Extension of this principle to other catalytic processes has so far not been reported.

Organosilanes bearing electron-withdrawing substituents[18] or incorporated into heterocyclic systems[19] behave as Lewis acidic activators or undergo reactions with organic carbonyls in the absence of added Lewis acid catalysts. It has also been demonstrated that trialkylsilyl triflates are able to catalyze a variety of organic reactions including aldol condensations.[20,21] In the latter case, the activity of the catalyst arises from the generation of silyl cations formed by dissociation of the silyl triflate species. Interestingly, trimethylsilyl iodide (TMSI) displays a similar activity.[22] As part of our general interest in the chemistry of Lewis acids, we became eager to establish whether trimethylsilyl chloride (TMSCl) could be activated to display a comparable activity. By analogy with the work carried out on the activation of group 4 metallocenes through anionic ligand abstraction by fluorinated Lewis acids,[5,6] we initiated a study focused on the activation of TMSCl with halophilic activators.[23] In this contribution, we report that the cyanosilylation of benzaldehyde is efficiently catalyzed by TMSCl in the presence of *o*-$C_6F_4(HgCN)_2$, which serves as a bidentate Lewis acid activator.

Results and Discussion

Synthesis and Characterization of the Mercury Derivatives. As part of these investigations and in order to compare their activities, we first synthesized a series of organomercury cyanide derivatives as halophilic activators. Organomercury chloride starting materials (**1**−**4**) were prepared according to literature procedures (Scheme 1).[24−26] These derivatives have been previously characterized, and several structures involving **1**[27−30] and **3**[31] have been reported. As part of this work, we obtained single crystals of **2** as a DMF adduct that were subjected to single-crystal X-ray analysis. [**2**·DMF] crystallizes in the tetragonal $P\text{-}4_2(1)$ space group with eight molecules in the unit cell (Figure 1, Table 1). With an approximately linear geometry (C(1)−Hg(1)−Cl(1) = 171.1(5)°, C(3)−Hg(2)−Cl(2) = 176.5(5)°), the coordination sphere of the mercury center resembles that of related derivates such as **3**·0.5(DMF).[31] The DMF ligand interacts with one of the two mercury centers with which it forms an Hg−O bond of 2.746(14) Å that is approximately perpendicular to the C−Hg−Cl sequence (O(1)−Hg(1)−Cl(1) = 92.2(3)°, O(1)−Hg(1)−C(1) = 96.3(6)°). With a terminal DMF ligand, the structure of [**2**·DMF] contrasts with that of **1**·μ_2-DMF, which features a μ_2-bridging oxygen bound DMF molecule.[27] This structural difference shows that unlike **1** and as a result of the 1,3-attachement of the mercury atom on the benzene ring, **2** is a nonchelating bifunctional Lewis acid.

Reactions of **1**−**4** with trimethylsilyl cyanide (TMSCN) afforded a high yield of the corresponding cyanide derivatives **5**−**8** (Scheme 1). These compounds have been characterized by elemental analysis, ^{1}H, ^{13}C, ^{19}F, and ^{199}Hg NMR, and IR spectroscopy. The infrared spectrum of these complexes displays a cyanide stretching band in the range 2170−2183 cm^{-1}, while their mercury chemical shifts are all within the range −1170 to −1250 ppm. The crystal structures of **5** and **8** have been determined by X-ray diffraction methods. Attempts to crystallize compound **5** from MeCN have so far been unsuccessful. In search of an adequate solvent, we chose acetaldehyde, which has been previously used to crystallize pure **1**.[30] Compound **5** dissolves in acetaldehyde and affords, upon slow evaporation, single crystals of the adduct [**5**·MeCOH]. This adduct crystallizes in the rhombohedral space group *R*-3 with six molecules in the

(18) Sakurai, H. *Synlett*. **1989**, 1−8. Marshall, J. A. *Chemtracts−Org. Chem*. **1998**, *11*, 697−712.
(19) Kinnaird, J. W. A.; Ng, P. Y.; Kubota, K.; Wang, X.; Leighton, J. L. *J. Am. Chem. Soc.* **2002**, *12*, 7920−7921, and reference therein.
(20) Carreira, E. M.; Singer, R. A. *Tetrahedron Lett*. **1994**, *35*, 4323−4326.
(21) Sugiura, M.; Hagio, H.; Hirabayashi, R.; Kobayashi, S. *J. Am. Chem. Soc.* **2001**, *123*, 12510−12517. Seeberger, P. H.; Haase, W.-C. *Chem. Rev.* **2000,** *100*, 4349−4394. Boons, G.-J.; Demchenko, A. V. *Chem. Rev.* **2000**, *100*, 4539−4566. Hanessian, S.; Lou, B. *Chem. Rev.* **2000**, *100*, 4443−4464. Graybill, T. L.; Casillas, E. G.; Pal, K.; Townsend, C. A. *J. Am. Chem. Soc.* **1999**, *121*, 7729−7746. Nishizawa, M.; Yamamoto, H.; Seo, K.; Imagawa, H.; Sugihara, T. *Org. Lett.* **2002**, *4*, 1947−1949. Evans, D. A.; Burgey, C. S.; Kozlowski, M. C.; Tregay, S. W. *J. Am. Chem. Soc.* **1999**, *121*, 686−699. Chen, J.; Sakamoto, K.; Orita, A.; Otera, J. *J. Org. Chem*. **1998**, *63*, 9739−9745. Murata, S.; Suzuki, M.; Noyori, R. *J. Am. Chem. Soc.* **1980**, *102*, 3248−3249. Mukai, C.; Hashizume, S.; Nagami, K.; Hanaoka, M. *Chem. Pharm. Bull*. **1990**, *38*, 1509−1512.
(22) Sakurai, H.; Sasaki, K.; Hosomi, A. *Bull. Chem. Soc. Jpn*. **1983**, *56*, 3195−3196. Miura, K.; Ootsuka, K.; Suda, S.; Nishikori, H.; Hosomi, A. *Synlett*. **2002**, *2*, 313−315.
(23) Fürstner, A.; Voigtländer, D. *Synthesis* **2000**, 959−969.
(24) For the synthesis of **1** see: Massey, A. G.; Al-Jabar, N. A. A.; Humphries, R. E.; Deacon, G. B. *J. Organomet. Chem*. **1986**, *316*, 25−39.
(25) For the synthesis of **3** see: Chambers, R. D.; Coates, G. E.; Livingstone, J. G.; Musgrave, W. K. R. *J. Chem. Soc.* **1962**, 4367−4371.
(26) For the synthesis of **2** and **4** see: Albrecht, H. B.; Deacon, G. B. *J. Organomet. Chem*. **1973**, *57*, 77−86. Deacon, G. B.; Tunaley, D. *J. Organomet. Chem*. **1978**, *156*, 403−426.
(27) Tschinkl, M.; Schier, A.; Riede, J.; Gabbai, F. P. *Organometallics* **1999**, *18*, 1747−1753.
(28) Tschinkl, M.; Bachman, R. E.; Gabbai, F. P. *Organometallics* **2000**, *19*, 2633−2636.
(29) Gardinier, J. R.; Gabbai, F. P. *J. Chem. Soc., Dalton Trans.* **2000**, 2861−2865.
(30) Beckwith, J. D.; Tschinkl, M. T.; Tsunoda, M.; Picot, A.; Gabbaï, F. P. *Organometallics* **2001**, *20*, 3169−3174.
(31) Tschinkl, M.; Schier, A.; Riede, J.; Gabbai, F. P. *Organometallics* **1999**, *18*, 2040−2042.

Table 1. Crystal Data, Data Collection, and Structure Refinement for 2·DMF, 8, 5·MeCOH, and 5·PhCOH

	2·DMF	**5**·MeCOH	**8**	**5**·PhCOH
		Crystal Data		
formula	$C_9H_7Cl_2F_4Hg_2NO$	$C_{11}H_4F_4Hg_2N_2O$	$C_7H_1F_4Hg_1N$	$C_{15}H_6F_4Hg_2N_2O$
M_r	693.24	657.34	375.68	707.4
cryst size (mm^3)	0.10 × 0.09 × 0.09	0.04 × 0.03 × 0.17	0.16 × 0.068 × 0.014	0.33 × 0.310 × 0.164
cryst syst	tetragonal	rhombohedral	monoclinic	monoclinic
space group	*P*-42(1)c	*R*-3	$P2_1/c$	*P*2(1)
a (Å)	18.9056(12)	15.418(3)	11.9823(8)	7.6177(5)
b (Å)	18.9056(12)	15.418(3)	7.8366(5)	7.5667(5)
c (Å)	7.5524(7)	15.418(3)	8.4287(6)	13.6722(10)
α (deg)	90	115.434(2)	90	90
β (deg)	90	115.434(2)	102.4250(10)	99.0700(10)
γ (deg)	90	115.434(2)	90	90
V ($Å^3$)	2699.4(3)	1967.6(6)	772.92(9)	778.22
Z	8	6	4	2
ρ_{calc} (g cm^{-3})	3.412	3.329	3.228	3.019
μ(Mo Kα) (mm^{-1})	23.152	23.421	19.928	19.751
F(000) (e)	2448	1728	664	628
		Data Collection		
T (K)	110(2)	110	110	110
scan mode	*ω*	*ω*	*ω*	*ω*
hkl range	-22→14, −22→21,−8→8	-12→17, −17→17,−17→15	-12→13, −8→8,−9→8	-8→9, −8→7,−16→16
no. of measd reflns	18 040	8962	4634	3148
no. of unique reflns, [R_{int}]	2361 [0.1076]	2046 [0.1403]	1206 [0.00829]	1785 [0.0398]
no. of reflns used for refinement	2361	2046	1206	1785
abs corr	empirical	empirical	empirical	empirical
$T_{min.}/T_{max.}$	0.4602/0.6607	0.1006/0.9891	0.2668/0.9989	0.1546/0.5877
		Refinement		
no. of refined params	172	172	118	217
R1, wR2 [$I>2\sigma(I)$]	0.0475, 0.1138	0.0.0678, 0.1541	0.0447, 0.1108	0.0297, 0.0793
ρ_{fin} (max./min.) (e $Å^{-3}$)	4.571, −1.421	5.936, −2.450	3.904, −1.524	2.076, −1.534

[a] $R1 = (F_o - F_c)/F_o$. [b] $wR2 = \{[w(F_o^2 - F_c^2)^2]/[w(F_o^2)^2]\}^{1/2}$; $w = 1/[\sigma^2(F_o^2) + (ap)^2 + bp]$; $p = (F_o^2 + 2F_c^2)/3$; $a = 0.02$ (**2**·DMF), 0.09 (**5**·MeCOH), 0.09 (**8**); 0.0703 (**5**·PhCOH); $b = 0$ (**2**·DMF), 100 (**5**·MeCOH), 6.6454 (**8**), 11.7377 (**5**·PhCOH).

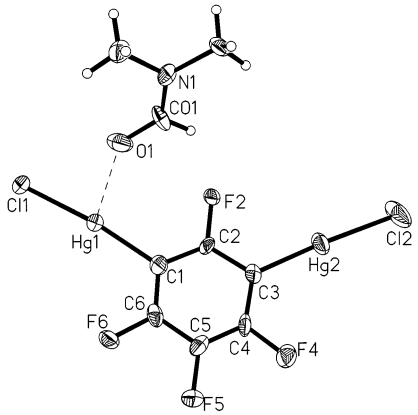

Figure 1. Structure of **2**·DMF in the crystal. ORTEP drawing (50%). Selected bond lengths [Å] and angles [deg]: Hg(1)−C(1) 2.062(18), Hg(1)−Cl(1) 2.321(4), Hg(1)−O(1) 2.746(13), Hg(2)−C(3) 2.008(17), Hg(2)−Cl(2) 2.295-(6), O(1)−C(01) 1.23(2), N(1)−C(01) 1.30(2), N(1)−C(03) 1.46(2), N(1)−C(02) 1.48(2), C(1)−Hg(1)−Cl(1) 171.5(5), C(1)−Hg(1)−O(1) 96.3(6), Cl(1)−Hg(1)−O(1) 92.2(3), C(3)−Hg(2)−Cl(2) 176.6(6), C(01)−O(1)−Hg(1) 134.0(13), C(01)−N(1)−C(03) 119.6(16), C(01)−N(1)−C(02) 123.8(16), O(1)−C(01)−N(1) 125.7(19).

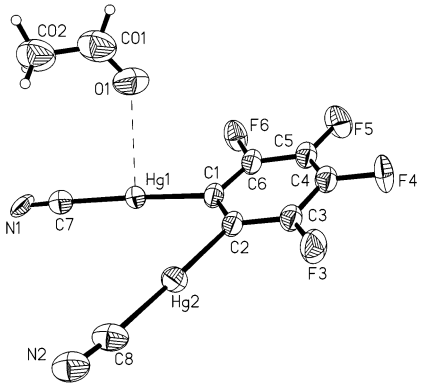

Figure 2. Structure of **5**·MeCOH in the crystal. ORTEP drawing (50%). Selected bond lengths [Å] and angles [deg]: Hg(1)−C(1) 2.05(2), Hg(1)−C(7) 2.07(3), Hg(1)−O(1) 2.855(19), Hg(2)−C(8) 2.08(2), Hg(2)−C(2) 2.10(2), O(1)−C(01) 1.19(4), N(1)−C(7) 1.11(3), N(2)−C(8) 1.13(3), C(01)−C(02) 1.46(5), C(1)−Hg(1)−C(7) 177.5(8), C(1)−Hg(1)−O(1) 87.2(7), C(7)−Hg(1)−O(1) 95.2(7), C(8)−Hg(2)−C(2) 178.4(8), C(01)−O(1)−Hg(1) 138(2), N(1)−C(7)−Hg(1) 178(2), N(2)−C(8)−Hg(2) 175(2), O(1)−C(01)−C(02) 125(3).

unit cell (Figure 2, Table 1). The structure reveals the existence of an acetaldehyde terminally bound to the mercury center at Hg(1). The resulting mercury−oxygen distance of 2.855(19) Å is longer than that encountered in adducts involving **1** and organic carbonyls such as acetone (2.679(13) and 2.776(14) Å)[27] and benzaldehyde (2.68(1) Å).[30] The C(1)−Hg(1)−C(7) (177.5(8)°) and C(8)−Hg(2)−C(2) (178.4(8)°) bond angles are, as expected, close to 180°. Molecules of [**5**·MeCOH] aggregate into hexamers whose shape is reminiscent of a capsule (Figure 3). The interactions responsible for the cohesion of this supramolecule involve the nitrogen terminus of each cyanide group that forms two long contacts with the mercury centers of a neighboring molecule. The resulting Hg···N distances (Table 2) are within the sum of the van der Waals radii for nitrogen ($r_{vdw} = 1.60$ Å)[32] and mercury (1.73−2.00 Å).[33] They are also similar to those observed in the known [**1**·μ_2-MeCN] (2.82(1) and

(32) Nyburg, S. C.; Faerman, C. H. *Acta Crystallogr. Sect. B* **1985**, *41*, 274−279.

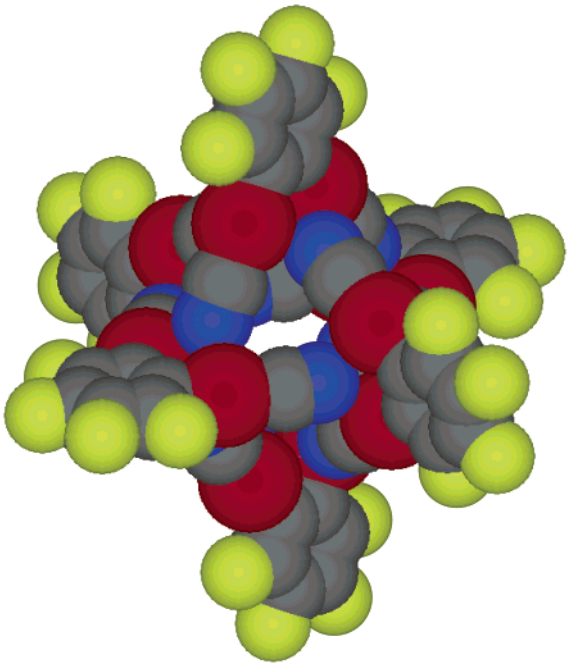

Figure 3. Space-filling model showing the hexameric aggregate formed in the solid-state structure of **5**·MeCOH. The acetaldehyde molecules have been omitted for clarity. Color code (F, green; C, gray; N, blue; Hg, red).

Table 2. Intermolecular Interactions Observed in 5·MeCOH and 8

Hg···N Interactions in **5**·MeCOH	
Hg(1)−N(1) = 3.018[a]	Hg(1)−N(2) = 2.899[b]
Hg(2)−N(1) = 2.831[a]	Hg(2)−N(2) = 2.832[b]
Hg···N and Hg···F Interactions in **8**	
Hg(1)−N(1) = 2.781[a]	Hg(1)−N(1) = 2.957[b]
Hg(1)−F(5) = 3.108[c]	Hg(1)−F(5) = 3.413[d]

[a] $-x+1, 0.5+y, 0.5-z$. [b] $x, 0.5-y, -0.5+z$. [c] $x, y-1, z$. [d] $x, -0.5-y, -0.5+z$.

2.93(1) Å).[30] This adduct rapidly decomposes into an opaque material through loss of the acetaldehyde component as shown by elemental analysis. IR studies carried out on a fresh sample reveal a detectable shift of the carbonyl stretching frequency (ν_{CO} = 1717 cm^{-1} vs ν_{CO} = 1727 cm^{-1} in pure acetaldehyde) that is apparently weakened by its coordination to the mercury center. The crystal structure of tetrafluorophenylmercury cyanide (**8**) has also been determined. Compound **8** crystallizes in the monoclinic space group $P2_1/c$ with four molecules in the unit cell (Table 1, Figure 4). As in [**5**·MeCOH], the coordination geometry of the mercury center is almost linear (C(1)−Hg(1)−C(01) 174.6(5)°). Examination of the packing structure reveals the existence of a network cross-linked via intermolecular Hg···N and Hg···F contacts (Table 2). The Hg···N bond lengths are similar to those found in [**5**·MeCOH] and [**1**·μ_2-MeCN].[30] It is also noteworthy that the Hg···F contacts encountered in the structure of **8** are comparable to those observed in the solid-state structure of other organomercurials bearing fluorinated rings.[30,34]

(33) Canty, A. J.; Deacon, G. B. *Inorg. Chim. Acta* **1980**, *45*, L225-L227. Pyykkö, P.; Straka, M. *Phys. Chem. Chem. Phys.* **2000**, *2*, 2489−2493.

(34) Tsunoda, M.; Gabbai, F. P. *J. Am. Chem. Soc.* **2000**, *122*, 8335−8336.

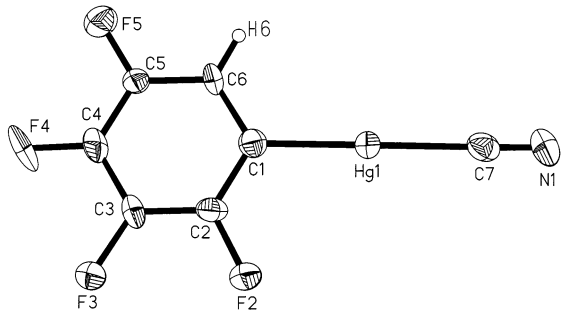

Figure 4. Structure of **8** in the crystal. ORTEP drawing (50%). Selected bond lengths [Å] and angles [deg]: Hg(1)−C(1) 2.030(11), Hg(1)−C(01) 2.067(13), N(1)−C(01) 1.139(16), C(1)−Hg(1)−C(01) 174.6(5), N(1)−C(01)−Hg(1) 177.6(11).

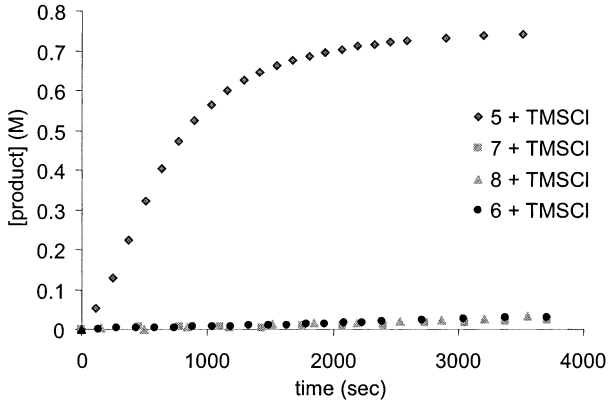

Figure 5. Plot showing the smooth conversion of benzaldehyde into phenyl(trimethylsiloxy)acetonitrile catalyzed by the combination of TMSCl and **5** compared to the reaction progress of the reaction catalyzed by TMSCl and a bifunctional Lewis acid, **6**, as well as monofunctional analogues **7** and **8**.

Scheme 2

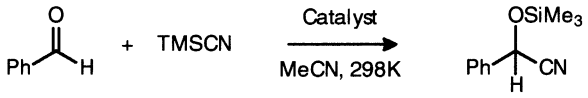

Table 3. Reaction Yields Obtained with Different Catalysts

entry	activator	[activator] mol %	yield
1	**5**	4.5	<5% after 30 min
2	**5** + TMSCl	4.5	97% after 30 min
3	**6** + TMSCl	4.5	<2% after 30 min
4	**7** + TMSCl	9.0	<3% after 30 min
5	**8** + TMSCl	9.0	<3% after 30 min
6	TMSCl	9.0	0% after 24 h
7	TMSBr	9.0	20% after 30 min
8	**5** + TMSBr	4.5	100% after 1 min

Catalysis. The reaction of benzaldehyde with 1.4 equiv of TMSCN in d_3-MeCN was monitored by ^{1}H NMR (Scheme 2, Table 3). On the time frame of our experiments, the reaction does not proceed in the absence of a catalyst or in the presence of **6**, **7**, and **8**. In the presence of the bidentate **5**, slow formation of the product is observed (entry 1). Interestingly, while the reaction does not proceed in the sole presence of TMSCl, the combination of TMSCl and compounds **5**−**8** leads to the formation of active catalytic species. Combination of **5** and TMSCl leads to a very active catalyst with 97% conversion after 30 min (entry 2, Figure 5). By contrast,

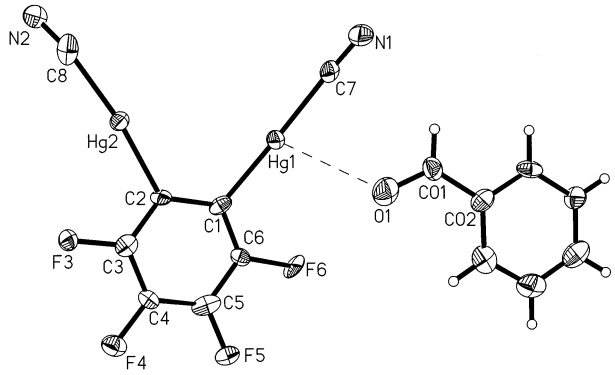

Figure 6. Structure of **5**·PhCOH in the crystal. ORTEP drawing (50%). Selected bond lengths [Å] and angles [deg]: Hg(1)−C(1) 2.060(17), Hg(1)−C(7) 2.075(16), Hg(1)−O(1) 3.009(12), Hg(2)−C(8) 2.088(13), Hg(2)−C(2) 2.057(13), O(1)−C(01) 1.27(2), N(1)−C(7) 1.14(2), N(2)−C(8) 1.12(2), C(01)−C(02) 1.44(2), C(1)−Hg(1)−C(7) 177.5(6), C(1)−Hg(1)−O(1) 104.5(5), C(7)−Hg(1)−O(1) 76.1(5), C(8)−Hg(2)−C(2) 172.5(7), C(01)−O(1)−Hg(1) 121.7(10), N(1)−C(7)−Hg(1) 174.9(13), N(2)−C(8)−Hg(2) 170.1(18), O(1)−C(01)−C(02) 123.7(15).

the use of compound **6**, a nonchelating bifunctional analogue of **5**, in combination with TMSCl leads to a much less active catalyst with only 4% conversion after 1 h (entry 3, Figure 5). The monofunctional derivatives **7** and **8**, which were used in 9 mol % in order to keep the total concentration in Lewis acid centers constant, also display a moderate activity (entries 4 and 5, Figure 5). These experiments show that the mercury cyanide derivatives alone display a very low catalytic activity. When combined with TMSCl, however, active catalytic species are formed, and the activity of bidentate **5** is superior to that of the nonchelating (**6**) or monofunctional derivatives (**7** and **8**).

In an effort to elucidate the obvious synergy operating between TMSCl and compound **5**, we attempted to study the order dependence of the reaction rate on the catalyst concentration. The reaction rate displays a first-order dependence both on TMSCl and on **5**, thus indicating that both of these compounds are involved in the rate-determining step and associated transition state. Attempts to isolate an adduct between **5** and benzaldehyde have been carried out. Slow evaporation of a benzaldehyde solution of **5** afforded single crystals of the adduct [**5**·PhCOH]. The crystals belong to the monoclinic space group *P*2(1) with two molecules in the unit cell. In this adduct, benzaldehyde acts as a terminal ligand and coordinates to only one mercury center (Figure 6). In **5**·PhCOH, the Hg(1)−O(1) bond of 3.009(12) Å is shorter than the sum of the van der Waals radii of oxygen (1.54 Å)[17] and mercury (1.73−2.00 Å).[18] It is however longer than the Hg−O distance (2.68(1) Å) observed in the structure of the related adduct [**1**·PhCOH], which also features a terminally bound aldehyde.[30] The carbonyl stretching frequency at 1694 cm^{-1} in [**1**·PhCOH] is close to that of pure benzaldehyde (ν_{CO} = 1701 cm^{-1}), which further substantiates the weakness of the Hg−O interaction.

It could be argued that the catalytic activity of the mixture **5**/TMSCl results from cyanide chloride exchange leading to the formation of TMSCN and **1**. If such was the case, compound **1**, by virtue of the greater electronegativity of the chloride ligand, would be expected to exhibit a greater Lewis acidity than **5** and could therefore directly activate the aldehyde. However, we noticed that reaction of **1** with TMSCN is quantitative and leads to **5** and TMSCl. Moreover, ^{199}Hg NMR of the reaction mixture sampled during a typical catalytic assay allowed for the detection of **5** only. In addition, we found that the combination of trimethylsilyl bromide (TMSBr) with **5** results in the formation of an extremely active catalytic species that surpasses the activity of the **5**/TMSCl mixture (entry 6). Since bromine is less electronegative than chlorine, a cyanide bromide exchange leading to the formation of 1,2-bis(bromomercurio)tetrafluorobenzene would yield a weaker bidentate Lewis acid and would not account for the activity of the **5**/TMSBr mixture. Interestingly, ESI/MS spectra of a mixture of **5** and TMSCl in MeCN in the anionic mode allowed for the detection of [**5**·Cl]$^-$ at m/z = 637 amu as the dominating species. The tetraphenylphosphonium salt of this anion, [**5**·Cl]$^-$[PPh_4]$^+$, can be isolated as a microcrystalline precipitate by diffusion of hexane into an equimolar solution of **5** and [PPh_4]$^+$$Cl^-$ in CH_2Cl_2.[35] These observations show that **5** readily complexes chloride anions. This conclusion is in agreement with the results obtained previously by Wuest on the complexation of chloride by nonfluorinated 1,2-bis(mercurio)benzenes.[9]

Scheme 3

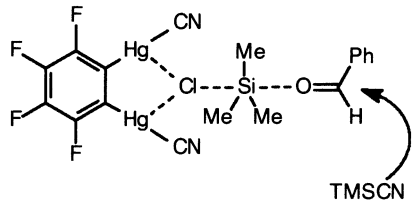

The catalytic activity observed with **5**−**8** in combination with TMSCl can be rationalized on the basis of a working model in which TMSCl is activated by the halophilic fluorinated mercury derivative (Scheme 3). Thus, the greater activity displayed by **5** can be correlated to its bidentate nature. Through complexation of the chloride and formation of a stable anionic chelate complex, compound **5** assists in the formation of the activated silicon species in a manner superior to the nonchelating activators **6**−**8**. In fact, while polydentate Lewis acids form stable halide complexes,[1,2] **6**−**8** are nonchelating and are expected to form rather labile terminal anionic complexes.[36] Efforts to observe the complex formation between **5** and TMSX (X = Cl^-, Br^-) in d_3-MeCN by ^{29}Si or ^{199}Hg NMR have been complicated by the coordinating ability of MeCN,[30] which presumably competes with the guest species. Hence, under the conditions of the reaction, the formation of the active silicon species can only be transient and thus unobservable.

Conclusions

The results presented in this study suggest that the catalytic activity of bidentate Lewis acid **5** in the cyanosilylation of benzaldehyde does not result from the

(35) Martin Tschinkl, Ph.D. Thesis, Technische Universität München, 1999.

(36) Goggin, P. L.; Goodfellow, R. J.; Hurst, N. W. *J. Chem. Soc., Dalton Trans.* **1978**, 561−566.

double electrophilic activation of benzaldehyde but rather involves the activation of a Lewis acidic silicon species that acts as a catalyst. On this premise, we note that a parallel exists between **5** and bidentate boranes that have been used as anion chelating activators of metallocene olefin polymerization catalysts.[5,6,12−17]

Experimental Section

General Considerations. ***Mercury compounds and especially $HgMe_2$ are highly toxic and should be handled with great care.*** All NMR studies were carried out on an Inova 400 MHz NMR spectrometer (400 MHz for ^{1}H, 100.5 MHz for ^{13}C, 71.56 MHz for ^{199}Hg). Neat $HgMe_2$ was used as an external standard for the solution ^{199}Hg NMR spectra. The proton and carbon signals of the deuterated solvent were used as internal standard for the ^{1}H and ^{13}C NMR spectra, respectively. ^{19}F NMR chemical shifts are reported relative to $CFCl_3$. All NMR spectra were recorded in acetone-d_6. IR spectroscopy studies were carried out in the solid state using KBr pellets on an ATI Matteson Genesis Series FTIR. MeCN and d_3-MeCN were distilled from CaH_2. Compounds **2**−**4** were prepared by following the literature procedures.[24−26]

Synthesis of *meta*-Bis(chloromercurio)tetrafluorobenzene (2). Compound **2** was prepared by a slightly modified version of the literature procedure.[26] HgO (8.45 g, 39.1 mmol) was added to a mixture of neat CF_3COOH (6 mL) and CF_3SO_3H (3 mL). Following the addition of a small amount of water (2 mL), 1,3,4,5-tetrafluorobenzene (1.5 g, 9.9 mmol) was added to the mixture. After stirring for 48 h, the resulting solution was reduced to dryness under vacuum. The residue was dissolved in MeOH and treated with HCl (2 mL, 12 M). Addition of water (75 mL) and cooling to 0 °C resulted in the precipitation of the product in 56% yield (3.43 g). ^{19}F NMR: δ −73.9, −113.1, 164.3. ^{13}C NMR: δ 121.2 (dd, $^2J_{F,C}$ = 45 Hz, $^2J_{F,C}$ = 59 Hz, *C*-1,3), 137.9 (d, $^1J_{F,C}$ = 253 Hz, *C*-2), 153 (d, $^1J_{F,C}$ = 239 Hz, *C*-4,6), 160.7 (d, $^1J_{F,C}$ = 225 Hz, *C*-5). Mp: 221 °C (dec). Anal. Calcd for $C_6F_4Cl_2Hg_2$: C, 11.62; H, 0.0. Found: C, 11.77; H, 0.0. Slow evaporation of a DMF solution yielded single crystals of the DMF adduct. These crystals were analyzed by X-ray diffraction methods.

Synthesis of the Organomercury Cyanide Derivatives (5−8). The organomercury cyanide derivatives were prepared in a glovebox by treatment of the corresponding organomercury chlorides (1 mmol) with a solution of TMSCN (4 mmol) in MeCN (3 mL). After complete dissolution of the solid, all volatiles were removed under vacuum and the resulting solid was evacuated overnight. This procedure yielded the pure organomercury cyanide derivatives **6**−**8**. In the case of **5**, the residue was washed with Et_2O to remove a small amount of impurity and the product was isolated by centrifugation.

***ortho*-Bis(cyanomercurio)tetrafluorobenzene (5).** IR (KBr pellet): ν 2182, 1653, 1617, 1590, 1479, 1457, 1426, 1419, 1322, 1295, 1090, 1010, 825, 775 cm^{-1}. ^{13}C NMR: δ 140.61 (d, $^1J_{F,C}$ = 259 Hz, *C*-3,6), 141.79 (d, $^2J_{F,C}$ = 33 Hz, *C*-1,2), 149.86 (d, $^1J_{F,C}$ = 230 Hz, *C*-4,5), 154.17 (CN). ^{19}F NMR: δ −116.5, −156.84. ^{199}Hg NMR: δ −1251. Mp: decomposes around 300 °C. Anal. Calcd for $C_8N_2F_4Hg_2$: C, 15.98; N, 4.66. Found: C, 15.81; N, 4.54.

***meta*-Bis(cyanomercurio)tetrafluorobenzene (6).** IR (KBr pellet): ν 2362, 2178, 1622, 1586, 1456, 1426, 1375, 1340, 1227, 1059, 1033, 879, 722. ^{13}C NMR: δ 123.7 (b, *C*-1,3), 138 (d, $^1J_{F,C}$ = 251 Hz, *C*-2), 153.7 (d, $^1J_{F,C}$ = 238 Hz, *C*-4,6), 163 (d, $^1J_{F,C}$ = 228 Hz, *C*-5), 153.8 (s, *C*N). ^{19}F NMR: δ −72.3, −112.74, 165.6. ^{199}Hg NMR: δ −1175. Mp: 280 °C (dec). Anal. Calcd for $C_8N_2F_4Hg_2$: C, 15.98; N, 4.66. Found: C, 16.12; N 4.60.

Pentafluorophenylmercury Cyanide (7). IR (KBr pellet): ν 2183, 1653, 1641, 1516, 1474, 1457, 1383, 1286, 1135, 1094, 1081, 813, 718, 668, 612 cm^{-1}. ^{13}C NMR: δ 137.8 (d, $^1J_{F,C}$ = 246 Hz, *C*-2,6 or *C*-3,5), 141.1 (d, $^1J_{F,C}$ = 242 Hz, *C*-4), 143.2 (b, *C*-1), 148.4 (d, $^1J_{F,C}$ = 242 Hz, *C*-2,6 or *C*-3,5), 151.84 (s, *C*N). ^{19}F NMR: δ −117.7, −118.99, −153.9, −161.0. ^{199}Hg NMR: δ −1212. Mp: 151−153 °C. Anal. Calcd for C_7NF_5Hg: C, 21.36; N, 3.56. Found: C, 21.58; N, 3.52.

***ortho*-Tetrafluorophenylmercury Cyanide (8).** IR (KBr pellet): ν 2920, 2170, 1621, 1602, 1520, 1506, 1451, 1350, 1317, 1291, 1278, 1204, 1184, 1120, 1087, 1030, 1000, 880, 811, 705 cm^{-1}. ^{1}H NMR: δ 7.42. ^{13}C NMR: δ 119 (td, $^2J_{F,C}$ = 34.53 Hz, *C*-6), 136.92 (d, $^2J_{F,C}$ = 44 Hz, *C*-1), 140.46 (d, $^1J_{F,C}$ = 249 Hz, *C*-3 or *C*-4), 140.55 (d, $^1J_{F,C}$ = 248 Hz, *C*-3 or *C*-4), 147.80 (d, $^1J_{F,C}$ = 248 Hz, *C*-2 or *C*-5), 150.04 (d, $^1J_{F,C}$ = 231 Hz, *C*-2 or *C*-5), 153.53 (s, *C*N). ^{19}F NMR: δ −117.9, −140.2, −156.6, −157.3. ^{199}Hg NMR: δ −1248. Mp: 171−174 °C. Anal. Calcd for C_7HNF_4Hg: C, 22.38; H, 0.27; N, 3.73. Found: C, 22.73; H, 0.35; N, 3.73.

General Procedure for the Catalytic Studies. In a typical experiment, benzaldehyde (0.1 g, 0.95 mmol) was rapidly added via a syringe to an NMR tube containing a d_3-MeCN solution (1.0 mL) of TMSCl (10.5 μL, 0.084 mmol), TMSCN (0.13 g, 1.3 mmol), and one of the catalysts (**5**, (0.025 g, 0.042 mmol) **6** (0.025 g, 0.042 mmol), **7** (0.033 g, 0.084 mmol), **8** (0.034 g, 0.084 mmol)). The small volume variation caused by the addition of benzaldehyde was negligible. ^{1}H NMR was utilized to monitor the disappearance of the aldehydic signal at 10.01 ppm and the appearance of the product signal at 5.74 ppm. The spectra were recorded at regular intervals in an automated fashion. Analysis was conducted by integration of the two monitored signals. The reaction advancement was plotted versus time for each catalyst. In the cases of **6**, **7**, and **8** when the catalysis proceeded very slowly, spectra were recorded hourly for 5 h.

Acknowledgment. Support from the National Science Foundation in the form of a CAREER award (CHE-0094264) and an equipment grant (CHE-9807975; purchase of the X-ray diffractometers) is gratefully acknowledged.

Supporting Information Available: Experimental details for the kinetic studies and X-ray crystallographic data for **2**·DMF, **8**, **5**·MeCOH, and **5**·PhCOH in CIF format. This material is available free of charge via the Internet at http://pubs.acs.org.

OM020918U